Research

New Phytologist

Bounds on stomatal size can explain scaling with stomatal density in forest plants

Congcong Liu[1,2,3]*, Christopher D. Muir[4]*, Lawren Sack[5], Ying Li[3], Li Xu[3], Mingxu Li[3], Jiahui Zhang[3], Hugo Jan de Boer[6], Xingguo Han[7], Guirui Yu[3] and Nianpeng He[8,9,10]

[1]Key Laboratory of Ecology and Environment in Minority Areas (Minzu University of China), National Ethnic Affairs Commission, Beijing, 100081, China; [2]College of Life and Environmental Sciences, Minzu University of China, Beijing, 100081, China; [3]Key Laboratory of Ecosystem Network Observation and Modeling, Institute of Geographic Sciences and Natural Resources Research, Chinese Academy of Sciences, Beijing, 100101, China; [4]Department of Botany, University of Wisconsin, Madison, WI 53706, USA; [5]Department of Ecology and Evolutionary Biology, University of California, Los Angeles, CA 90025, USA; [6]Copernicus Institute of Sustainable Development, Department of Environmental Sciences, Utrecht University, Utrecht, 80125, the Netherlands; [7]State Key Laboratory of Vegetation and Environmental Change, Institute of Botany, Chinese Academy of Sciences, Beijing, 100093, China; [8]Key Laboratory of Boreal Forest Ecosystem Conservation and Restoration, National Forestry and Grassland Administration, Harbin, 150040, China; [9]Institute of Carbon Neutrality, School of Ecology, Northeast Forestry University, Harbin, 150040, China; [10]Earth Critical Zone and Flux Research Station of Xing'an Mountains, Chinese Academy of Sciences, Daxing'anling, 165200, China

Authors for correspondence:
Nianpeng He
Email: henp@igsnrr.ac.cn

Christopher D. Muir
Email: cdmuir@wisc.edu

Received: *9 June 2025*
Accepted: *11 September 2025*

New Phytologist (2025) **248:** 2910–2926
doi: 10.1111/nph.70626

Key words: evolution, forests, maximum stomatal conductance, stomatal density, stomatal size, trade-off.

Summary

- A prevailing hypothesis posits that achieving higher maximum rates of leaf carbon gain and water loss is constrained by geometry and/or selection to limit the allocation of epidermal area to stomata (f_S). Under this 'stomatal-area minimization hypothesis', higher $g_{s,max}$ is associated with greater numbers of smaller stomata because this trait combination increases $g_{s,max}$ with minimal increase in f_S, leading to relative conservation of f_S semi-independent of $g_{s,max}$ due to coordination in stomatal size, density, and pore depth. An alternative hypothesis is that the evolution of higher $g_{s,max}$ can be enabled by a greater epidermal area allocated to stomata, leading to positive covariation between f_S and $g_{s,max}$; we call this the 'stomatal-area adaptation hypothesis'. Under this hypothesis, the interspecific scaling between $g_{s,max}$, stomatal density, and stomatal size is a by-product of selection on a moving optimal $g_{s,max}$.
- We integrated biophysical and evolutionary quantitative genetic modeling with phylogenetic comparative analyses of a global data set of stomatal density and size from 2408 vascular forest species. The models present specific assumptions of both hypotheses and deduce predictions that can be evaluated with our empirical analyses of forest plants.
- There are three main results. First, neither the stomatal-area minimization nor adaptation hypothesis is sufficient to be supported. Second, estimates of interspecific scaling from common regression methods cannot reliably distinguish between hypotheses when stomatal size is bounded. Third, we reconcile both hypotheses with the data by including an additional assumption that stomatal size is bounded by a wide range and under selection; we refer to this synthetic hypothesis as the 'stomatal adaptation + bounded size' hypothesis.
- This study advances our understanding of scaling between stomatal size and density by mathematically describing specific assumptions of competing hypotheses, demonstrating that existing hypotheses are inconsistent with observations, and reconciling these hypotheses with phylogenetic comparative analyses by postulating a synthetic model of selection on $g_{s,max}$, f_S, and stomatal size.

Introduction

Stomatal pores are critical determinants of the function of plants and the composition of the atmosphere (Berry *et al.*, 2010). The stomatal conductance to diffusion of water vapor and CO_2 (g_s) influences a broad spectrum of ecological processes at leaf, community, and ecosystem scales, including photosynthesis, net primary production, and water-use efficiency (Cramer *et al.*, 2001; Haworth *et al.*, 2011). Stomata can regulate g_s either through evolutionary or plastic shifts in stomatal size or density (Jordan *et al.*, 2015) or through short-term stomatal aperture changes (Hetherington & Woodward, 2003). The g_s, and its typical operational value measured under field conditions ($g_{s,op}$), can thus vary from near zero with stomata fully closed to $g_{s,max}$

*These authors contributed equally to this work.

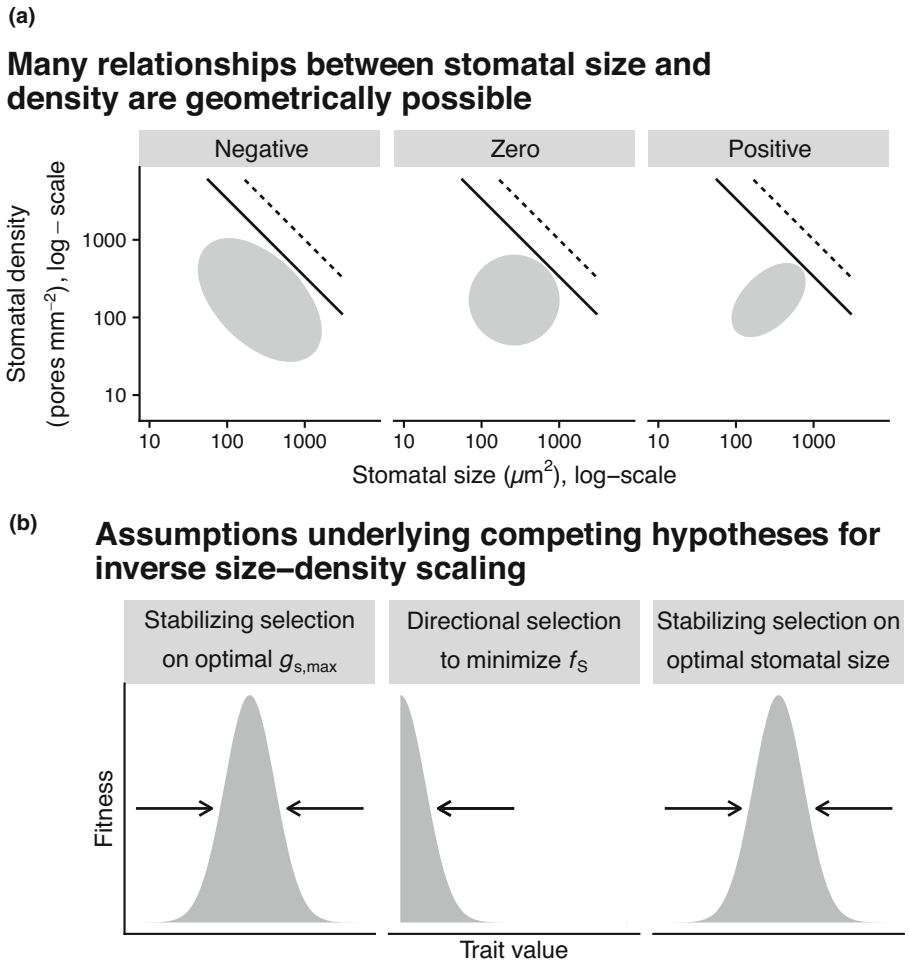

Fig. 1 Assumptions underlying competing hypotheses for stomatal size–density scaling make different predictions about the trait covariance structure. Maximum stomatal conductance ($g_{s,max}$) and the fraction of epidermal area allocated to stomata (f_S) are determined by stomatal density and size. On a log scale, they are the sum of log-stomatal density (d_S) and log-stomatal size (a_S) times a scaling exponent (β), 0.5 for $g_{s,max}$ and 1.0 for f_S (see the Materials and Methods section). (a) Many scaling relationships between stomatal size and density are possible as long as f_S does not exceed 1 (dashed line) or more realistically a value less than 1 to allow space between stomata (solid line, $f_S = 0.34$, the maximum value in our data set). The gray ellipses represent different possible scaling relationships with the same mean trait values in our data set ($\overline{A}_S = 263$ μm^2, $\overline{D}_S = 168$ pores mm^{-2}). These are 95% quantile of covariance ellipses for a bivariate normal with trait correlations of −0.5, 0, and 0.5 and trait variances of 0.75, 0.55, and 0.45 for 'negative', 'zero', and 'positive' relationships, respectively. (b) We consider nested hypotheses (see the Materials and Methods section) that all assume stabilizing selection on optimal $g_{s,max}$ (left panel) and then add complexity by assuming selection to minimize f_S (middle panel) and stabilizing selection on stomatal size (right panel).

with stomata fully open. The $g_{s,max}$ is a fundamental anatomical constraint, and across species measured under controlled conditions, $g_{s,op}$ and $g_{s,max}$ are correlated (Wilson, 1975; Franks *et al.*, 2013; Haworth *et al.*, 2013). For example, in woody angiosperms, $g_{s,op}$ is consistently *c.* 25% of $g_{s,max}$ (Murray *et al.*, 2020). Because of its importance in controlling leaf water and CO_2 fluxes, stomatal anatomy can provide critical information in global vegetation and crop models toward the current grand challenge of understanding how crops and forest trees are optimized for carbon gain vs water use (Ordoñez *et al.*, 2009; Yuan & Chen, 2009; Díaz *et al.*, 2016; Freschet *et al.*, 2017). The $g_{s,max}$ varies substantially among extant species (Sack & Buckley, 2016; Murray *et al.*, 2020; Liu *et al.*, 2022) and changed over geological time in response to global climate change (Royer, 2001; Franks *et al.*, 2009; McElwain & Steinthorsdottir, 2017). Trade-offs between carbon gain and costs of stomata, such as water loss, likely contribute to much of the variation in $g_{s,max}$ among extant species and over time, yet the relative importance of different costs among vascular land plants is not well-understood.

The $g_{s,max}$ is often modeled as a function (Eqn 2) of underlying anatomical traits stomatal density (D_s, number of pores per unit epidermal area) and size (A_s, area of guard cells surrounding each pore). The relationship between stomatal anatomy and conductance is derived from Fick's law of diffusion, with 'end-correction' albeit with simplifying assumptions about guard cell geometry and homogeneity of the leaf lamina. Anatomical traits are widely used to study the adaptation and competition of plants because they correlate with $g_{s,op}$ (Brown & Escombe, 1901; Parlange & Waggoner, 1970; Franks & Farquhar, 2001; Vatén & Bergmann, 2012; McElwain *et al.*, 2016; Conesa *et al.*, 2019; Murray *et al.*, 2020). Two long-standing observations about stomatal anatomy are that (1) A_s and D_s negatively covary and (2) higher $g_{s,max}$ is associated with greater density of smaller stomata among species. Both patterns have been observed among extant species and in the fossil record. Similar patterns often occur within species (e.g. Franks & Beerling, 2009a,b, and references therein). Biologists have long observed an inverse relationship between A_s and D_s across diverse plant species, first recognized in 1865 (Weiss, 1865), and well-established more recently (Franks & Beerling, 2009a; de Boer *et al.*, 2016; Sack & Buckley, 2016; Haworth *et al.*, 2023; Liu *et al.*, 2023). More recent surveys also observe that species with the greatest $g_{s,max}$ are on the high-D_s, low-A_s end of the spectrum (Franks & Beerling, 2009a; de Boer *et al.*, 2016). One might think that stomatal size and density negatively covary because of the geometric constraint that they cannot occupy more than the entire leaf surface, but this is not mathematically required (Fig. 1a). Evolutionary processes that affect stomata may result in predictable among-species scaling

exponents between size, density, and other traits (de Boer *et al.*, 2016).

Here, we consider two potential evolutionary hypotheses that are not mutually exclusive, but rather two endpoints along a continuum of explanations. The first hypothesis posits that epidermal space allocated for stomata is strongly constrained by selection maintaining other structures such as trichomes (Baird *et al.*, 2024) or bundle sheath extensions (Baresch *et al.*, 2019), or limiting pathogen infection (Muir, 2020), or maximizing internal leaf space for mesophyll cells (Lundgren *et al.*, 2019). Hence, there is likely a trade-off between allocating epidermal area to stomata, denoted f_S (Eqn 1), instead of other functions. The costs of allocating more stomatal area may increase as f_S increases because stomata crowd out other functions and even compromise the function of other stomata through stomatal interference (Lehmann & Or, 2015) and inadequate spacing to allow proper opening (Dow *et al.*, 2014). We refer to this as the 'stomatal-area minimization hypothesis' because it assumes that $g_{s,max}$ is constrained by selection to minimize f_s. This hypothesis is not new. For example, Franks *et al.* (2009) proposed that competition for epidermal space would predict that f_S should be relatively constant and D_S and A_S do not positively covary. Our goal for this hypothesis was to clarify its assumptions of this hypothesis and more completely derive its predictions.

One consequence of stomatal-area minimization is that a response to selection for sufficiently high $g_{s,max}$ can only be achieved through combinations of small stomata at high density (Franks & Beerling, 2009b). Because of the allometry between stomatal size and pore depth (de Boer *et al.*, 2016; Sack & Buckley, 2016), combinations of larger stomata at lower density with the same $g_{s,max}$ require more epidermal space than combinations of smaller stomata at higher density. This hypothesis could therefore explain why high $g_{s,max}$ leaves are associated with small stomata at high density. It can also explain why there is negative covariation between stomatal size and density. Leaves with the highest $g_{s,max}$ values cannot obtain certain combinations of larger size and lower density without increasing f_S beyond its geometric limit. However, it is not clear under this hypothesis why there appears to be a deficit of leaves with small size at low density (Fig. 1).

There are two potential problems with the stomatal-area minimization hypothesis. The first is that actual f_s is typically far below its geometric limit of 100% (33.6%) is the maximum f_s in our data set of extant species (Cornelissen *et al.* 2003; solid line in Fig. 1a) and most leaves are well below this (the median f_s is 4.4% in our data; see the 'Stomatal trait data from global forests' in the Materials and Methods section, for a description of the data). Compared with other geological periods, the f_S among extant leaves is relatively high because extant species evolved in a low-CO_2 world, current anthropogenic emissions notwithstanding, where carbon limitation is likely. It seems unlikely that space allocated to stomata would trade off with other epidermal functions when f_S values are this low. We are not questioning whether stomata have no cost (we discuss these costs later), but rather the assumption that epidermal space imposes a major limitation on stomatal trait variation. At prevailing values of f_S, most species could increase $g_{s,max}$ through higher A_s, D_s, or both; increasing $g_{s,max}$ does not require that A_s and D_s evolve in the opposite direction to minimize f_s (Franks *et al.*, 2009). For example, consider two leaves with stomatal densities 250 and 200 pores mm^{-2} and stomatal areas 150 and 187.5 μm^2. We use the following equations to calculate f_s and $g_{s,max}$ from A_s and D_s:

$$f_S = D_S A_S \quad \text{Eqn 1}$$

$$g_{s,max} = bmD_S A_S^{0.5} \quad \text{Eqn 2}$$

where b and m are biophysical and morphological constants, respectively (Sack & Buckley, 2016) (see the Materials and Methods section for equations to calculate these constants). The two leaves have an identical f_S of 0.0375, but $g_{s,max}$ at 25°C is 11% greater for the leaf with smaller stomata (1.47 vs 1.32 mol m^{-2} s^{-1}). Suppose the environment for the species with larger stomata (lower $g_{s,max}$) changed such that the optimal $g_{s,max}$ becomes 1.47 mol m^{-2} s^{-1}, how would this species respond to selection? It could respond by increasing D_S to 224 pores mm^{-2}, which would change f_S to 0.042, or it could respond by increasing A_S to 234 μm^2 and f_S to 0.047. To minimize f_S, selection for higher $g_{s,max}$ should favor higher D_S on the assumption that differences in f_S impose a fitness cost. We are not aware of empirical estimates of the selection gradient on f_S, and this will be an important area for future research.

A second potential problem with the stomatal-area minimization hypothesis is that directional selection for decreased f_S would eliminate variation in stomatal size. In the absence of any trade-offs on epidermal space allocated to stomata, the response to selection for higher $g_{s,max}$ depends on genetic (co)variance in stomatal size and density (Lande, 1979). When f_S is limited because of trade-offs, this manifests as a greater pleiotropic fitness cost of achieving high $g_{s,max}$ by increasing A_S and a lower pleiotropic fitness cost of achieving high $g_{s,max}$ by increasing D_S. A logical extension of this hypothesis is that even stabilizing selection on $g_{s,max}$ should favor greater D_S and lower A_S to minimize f_S. Unless genetic variance in D_S is near zero or there is strong positive genetic covariance between A_S and D_S, selection will favor smaller A_S. Such directional selection eventually eliminates variance, which contrasts with the wide variance in stomatal size among species. Responses to selection for smaller stomata to reduce f_S may be limited by factors such as genome size (Beaulieu *et al.*, 2008; Šímová & Herben, 2012; Roddy *et al.*, 2020) or inefficient diffusion through small pores (Hodgson *et al.*, 2010).

An alternative to the 'stomatal-area minimization' hypothesis is what we call the 'stomatal-area adaptation' hypothesis, that is f_S should evolve to optimize $g_{s,max}$. We assume that the optimal $g_{s,max}$ is determined by trade-offs between carbon gain, water loss, protection from pathogens, and other factors. In one sense, it is trivially true that the covariance between $g_{s,max}$ and f_S is almost certainly positive because both depend on stomatal density and size, which is borne out in our data set (Supporting Information Fig. S1). Mathematically, negative covariance between $g_{s,max}$ and f_S is only possible if the correlation between D_S and A_S is very

close to −1 (Notes S1), which is inconsistent with observations. Instead, what we mean is that selection for higher $g_{s,max}$ is much stronger than selection to minimize f_S, meaning that the response to selection will not be biased in the direction of minimizing surface allocation. This hypothesis recognizes that no relationship between A_s and D_s is mathematically required. If the fraction of the leaf surface taken up by stomata is much less than unity, qualitatively different relationships between stomatal size and density across species are geometrically possible, including negative, zero, and positive covariances (ellipses in Fig. 1a). Empirically, inverse scaling is common but not universal (Dunbar-Co *et al.*, 2009). The hypothesis also assumes that stomatal size and density can evolve at least somewhat independently within and among species. Stomata are spaced out by epidermal cells to open and close properly (Dow *et al.*, 2014), but the development of higher D_s can occur through the increased differentiation of epidermal cells into stomata (i.e. achieving higher stomatal differentiation rate, or stomatal index; Salisbury, 1928; Sack & Buckley, 2016), without any effect on stomatal size. Hence, A_s and D_s should be able to evolve independently. Empirically, populations can have genetic variation in stomatal size that is independent of genetic variation in density (e.g. Dittberner *et al.* (2018)). Under the stomatal-area adaptation hypothesis, many combinations of A_s and D_s have similar fitness through their effect on $g_{s,max}$ and the covariance between A_s and D_s among species emerges indirectly through their effect on $g_{s,max}$. This hypothesis is an oversimplification because not all A_S values are possible or adaptive. Genome size and physics limit stomata from becoming too small, as mentioned in the previous paragraph, and large stomata may be inefficient in terms of adjusting aperture because of their low surface area to volume ratio (Drake *et al.*, 2013; Raven, 2014).

Distinguishing between these hypotheses will help better understand changes in stomatal traits in the fossil record and variation among species and communities today. The stomatal-area minimization hypothesis indicates that competition for epidermal space is essential for understanding variation in stomatal traits. By contrast, the stomatal-area adaptation hypothesis indicates that selection on optimal $g_{s,max}$ is fundamental to understanding variation in stomatal traits. These are not mutually exclusive hypotheses. Stomatal-area minimization may be important as f_S approaches an upper bound, but the stomatal-area adaptation hypothesis may better explain variation when f_S is near zero.

Although multiple approaches are needed to evaluate these hypotheses, here we focus on among-species scaling between stomatal size and density. Because stomatal-area minimization and adaptation hypotheses assume different constraints on stomatal anatomy, they may result in different scaling relationships. Note that both f_S (Eqn 1) and $g_{s,max}$ (Eqn 2) show similar mathematical dependence on D_S and A_S that we can generalize as:

$$Z_S = Z_0 D_S A_S^{\beta} \qquad \text{Eqn 3}$$

where a composite stomatal trait Z_S (i.e. f_S or $g_{s,max}$) is proportional to the product of constituent stomatal traits (A_s and D_s), with scaling exponent β multiplied by a scalar Z_0, which reflects stomatal dimension proportionalities and physical diffusion factors (Sack & Buckley, 2016). For $g_{s,max}$, $Z_0 = bm$ and $\beta = 0.5$ (Eqn 1); for f_S, $Z_0 = 1$ and $\beta = 1$ (Eqn 2). The different scaling exponents arise because diffusion is proportional the linear dimension of the pore and the relationship between maximum pore area and depth is constrained by a relatively constant guard cell shape. Specifically, the length, width, and depth of guard cells are proportional, which is captured by the morphological constant described in more detail later. The different scaling exponents set up the potential for $g_{s,max}$ to increase semi-independently of f_S when plants evolve smaller and shallower stomata while stomatal density increases.

Since all traits are log-normally distributed, we log-transformed Eqn 3:

$$z_S = z_0 + d_S + \beta a_S \qquad \text{Eqn 4}$$

where lowercase variables indicate log-transformation of uppercase counterparts. Log-transformation also has the advantage of linearizing the equation, and traits measured on different scales can be directly compared in terms of proportional changes.

It is tempting to think that stomatal-area minimization and adaptation hypotheses could be tested by estimating the scaling exponent β among species. For the composite stomatal trait z_S to remain relatively constant among species that vary in d_S and a_S, the slope between d_S and a_S would need to be $-\beta$, which can be estimated using linear regression. For example, de Boer *et al.* (2016) estimated a scaling exponent close to unity, in that the standardized major axis (SMA) slope between stomatal density and size on a log–log scale was close to −1. They interpret this as evidence that species have diversified along an axis that increases $g_{s,max}$ with minimum increase in f_S. There are two potential problems with this interpretation. First, since the seminal evolutionary quantitative genetic (EQG) theory of Lande (1979), biologists have recognized that the among-species covariance does not necessarily map directly onto within-species covariance or short-term responses to selection. A second challenge is estimating scaling exponents because different methods, most commonly ordinary least-squares (OLS) and SMA regression, yield different estimates that may not support the same hypothesis. There is broad consensus that the choice of estimation procedure should be guided primarily by biological rather than by statistical considerations.

To resolve these problems and advance our understanding of the selective forces that underlie inverse stomatal size–density scaling in vascular land plants, it requires not only data but also theory. Mathematical models generate quantitative predictions and inform statistical decisions. The hypotheses for size–density scaling are based on responses to selection within species, but many studies analyze patterns among species. It is not clear how among species patterns map onto within species processes. EQG is especially well-suited to address this gap in our understanding because it explicitly bridges micro- and macroevolutionary scales (Arnold *et al.*, 2001). Models also inform whether OLS, SMA, or neither can estimate desired parameter values under competing

hypotheses. Theory helps empiricists gain biological insight by selecting statistical methods appropriate for the biological questions. Further background information on EQG and regression methods is provided in Notes S2. The five primary objectives in this study:

(**1**) provide specific mathematical assumptions about selection on stomatal density and size under the stomatal-area minimization and adaptation hypotheses;

(**2**) deduce the mean and expected genetic (co)variance between stomatal density and size within species at equilibrium (mutation-selection balance) under both stomatal-area minimization and adaptation hypotheses, as well as a new extended hypothesis we call the 'stomatal adaptation + bounded size' hypothesis (see the Materials and Methods section);

(**3**) deduce the short-term response to selection on $g_{s,max}$ based on the equilibrium genetic (co)variance between stomatal density and size within species under competing hypotheses;

(**4**) deduce the expected among-species (co)variance between stomatal density and size at stationarity using the Ornstein–Uhlenbeck (OU) model; and

(**5**) compare expected parameter values under different hypotheses to observed values estimated using a phylogenetic comparative data set of 2408 vascular forest plant species.

Materials and Methods

Assumptions of competing hypotheses

>To ground our hypotheses in EQG theory, we assume different individual fitness functions for each hypothesis. Under the stomatal-area adaptation hypothesis, we assume that log-$g_{s,max}$ is under stabilizing selection around an optimal log-$g_{s,opt}$:

$$W = W_{max}\exp\left(-\frac{\left(\log g_{s,max}-\log g_{s,opt}\right)^2}{2\omega}\right) \quad \text{Eqn 5}$$

where W is absolute fitness, W_{max} is the maximum absolute fitness, and ω is inversely proportional to the strength of selection. The $g_{s,opt}$ is the optimal value of $g_{s,max}$. We do not explicitly model demography; hence, only the relative fitness determines the change in trait frequency. Therefore, we can ignore W_{max} because it cancels out (i.e. we are assuming soft selection). Fitness is modeled as a Gaussian function because this is the simplest, most general, and mathematically tractable form of stabilizing selection and, therefore, widely used in EQG (Walsh & Lynch, 2018). As with many metric traits, the stomatal traits we consider are normally distributed on a log-transformed scale; therefore, we analyze log-transformed values throughout. The above assumptions about soft selection, the functional form of stabilizing selection, and log-transformation apply to all hypotheses.

One further, essential assumption that applies to all models is that $g_{s,opt}$ is not static, but changes dynamically through time, independently in every species. The specific mathematical assumptions are described later with additional detail in Notes S3. One key point to emphasize here is that we are not attempting to model the changes in the environment and/or other traits that cause $g_{s,opt}$ to fluctuate. Rather, our treatment is phenomenological and additional analysis would be required to determine how $g_{s,opt}$ responds to specific factors.

The additional assumption specific to the stomatal-area minimization hypothesis is that there is selection for decreased f_S, all else being equal:

$$W = W_{max}\exp\left(-\frac{\left(\log f_S-\log f_{S,min}\right)^2}{2\varphi_f\omega} - \frac{\left(\log g_{s,max}-\log g_{s,opt}\right)^2}{2\omega}\right) \quad \text{Eqn 6}$$

Although Eqn 6 appears to imply stabilizing selection on log f_S, it results in directional selection for lower f_S if $f_{S,min}$ is sufficiently low relative to $g_{s,opt}$ (see the Results section). Pure directional selection on f_S, in the absence of countervailing constraints on stomatal size, leads to selection for infinitesimal stomatal size and infinite stomatal density. The strength of selection on f_S relative to $g_{s,opt}$ is determined by φ_f, where values above unity indicate weaker selection on f_S than $g_{s,opt}$. In our formulation, the stomatal-area adaptation hypothesis is a special case of the stomatal-area minimization hypothesis, where $\varphi_f = \infty$. Hence, there is a continuum between these hypotheses modulated by φ_f, where lower values indicate stronger selection on minimized f_S relative to optimizing $g_{s,opt}$.

As described in the Results section and Tables 1 and 2, both hypotheses make predictions that are inconsistent with data from vascular land plants. In particular, the lack of constraint on stomatal size leads to unrealistic interspecific variation in this trait. It is therefore necessary to add an additional assumption about physical bounds on stomatal size, which we do by assuming stabilizing selection around an optimal stomatal size $a_{S,opt}$:

$$W = W_{max}\exp\left(-\frac{f_S}{2\varphi_f\omega}-\frac{\left(\log a_S-\log a_{S,opt}\right)^2}{2\varphi_a\omega} - \frac{\left(\log g_{max}-\log g_{s,opt}\right)^2}{2\omega}\right) \quad \text{Eqn 7}$$

We refer to this extended model as the 'stomatal adaptation + bounded size' hypothesis. In contrast to Eqn 6, pure directional selection of f_S does not lead infinitesimal stomatal size because of the stabilizing selection term in Eqn 7. It is not an alternative model because the first two models are nested within this more complex model. In this model, directional selection for lower f_S is limited by stabilizing selection on both stomatal size and $g_{s,max}$. While we do not explicitly model the fitness costs of extreme

Table 1 Assumptions and microevolutionary predictions of competing hypotheses for the scaling of stomatal size and density.

	Assumptions		Microevolutionary equilibria within species		Response to selection on $g_{s,max}$
Hypothesis	Fitness function	Fluctuating fitness optima	Trait means	Genetic (co)variance	Trait response
H_1: Stomatal-area adaptation	Eqn 5	$g_{s,max}$	Neutrally stable (Eqn S32)	Infinite variance (S3.3.1.5)	Density responds more Covariance always negative (Figs S8–S10)
H_2: Stomatal-area minimization	Eqn 6	$g_{s,max}$	Stable (Eqn S49)	Finite variance (S3.3.2.5)	Variable trait response and covariance (Figs S8–S10)
H_3: Stomatal adaptation + bounded size	Eqn 7	$g_{s,max}$ and A_S	Stable (Eqn S61)	Finite variance (S3.3.3.5)	Variable trait response Covariance usually positive (Figs S8–S10)

The hypotheses start by making different assumptions about the relationship between stomatal traits and fitness and which fitness optima fluctuate through time. The models differ in whether they predict within-species trait means that are neutrally stable or stable. The equation number in parentheses cross references the relevant part of the Supporting Information. The genetic (co)variance matrix between stomatal density and size can be infinite or finite. The section number in parentheses cross references the relevant part of the Supporting Information. Finally, responses to selection on $g_{s,max}$ can change primarily stomatal density, size, or both. Furthermore, the covariance in density and size responses can be positive, near zero, or negative. Variable response means that the predictions are sensitive to microevolutionary parameters such as mutational variance and the strength of selection. Cross-referenced figures in the Supporting Information illustrate these conclusions.

stomatal size, there are good reasons to suppose stomatal size must vary within limits (see the Discussion section). The parameter φ_a modulates the strength of stabilizing on stomatal size per se relative to the strength of selection on $g_{s,max}$. In this model, we first treat $a_{S,opt}$ as a constant, but this predicts zero variance in stomatal size at equilibrium (Eqn S64 in the Supporting Information shows that there is no variation stomatal size when there is a fixed optimum). Hence, it is necessary to model $a_{S,opt}$ as a variable in the same manner as $g_{s,opt}$.

Trait mean and genetic (co)variance equilibria within species

With the assumed fitness functions described previously, we analyzed each hypothesis using the Lande's (1979) equations for the short-term change in the trait mean vector and the additive genetic covariance and solved for the equilibria in which the short-term change equals zero. For the stomatal-area adaptation hypothesis, we obtained analytical solutions; for the remaining hypotheses, we solved the equilibria numerically over a range of relevant parameter space. Detailed derivations of all equilibria are given in Notes S3.

Short-term responses to selection on $g_{s,max}$ within species

We used the equilibrium genetic (co)variance matrix from each hypothesis to predict the vector of evolutionary responses in stomatal density and size when there is selection for greater $g_{s,max}$ for plausible parameter values described in Notes S3. A vector that increases a_S-only minimizes the increase in f_S, a vector that increases d_S-only maximizes the increase in f_S, and vectors that increase a_S and d_S simultaneously are intermediate. We compared the angle of the vector of responses to the angle predicted for the interspecific covariance and that observed in our data set. The analogous vectors for selection on lower $g_{s,max}$ are simply the reverse sign of those for greater $g_{s,max}$. We treated d_S and a_S as quantitative traits evolving in multivariate Gaussian populations (Walsh & Lynch, 2018) subject to selection and mutation. Hence, we assume that population sizes are sufficiently large to ignore genetic drift, random mating within species is panmictic, and there is no gene flow between species. A complete description of all model variables is given in Notes S3.

Trait mean and (co)variance among species at stationarity

We assume that over macroevolutionary time, $\log(g_{s,opt})$ fluctuates stochastically and independently in all species following a univariate or multivariate OU process. With sufficient time, an OU process evolves to a stationary mean equal to the long-run average denoted θ. This is the average trait value among species at stationarity. The fluctuations in the adaptive optimum have a SD σ and the 'pull' back toward θ is controlled by the parameter α. The stationary trait variance among species is determined by σ and α parameters. Under the stomatal-area adaptation, stomatal-area minimization, and stomatal adaptation + bounded size (static $a_{S,opt}$) hypotheses, we assume that only $\log(g_{s,opt})$ varies through time; the parameters governing selection for lower f_S and optimal stomatal size are assumed constant in these models. If the strength of selection on these traits varied through time, but the average strength was constant, the parameters can be interpreted as the geometric mean. If the selection parameters were changing through time on average, then our assumption that the distribution is stationary would be violated. We also considered a multivariate OU version of the stomatal adaptation + bounded size model with fluctuating $a_{S,opt}$. In this model, $g_{s,opt}$ and $a_{S,opt}$ fluctuate simultaneously either independently or with some correlation. The parameters for the multivariate OU extend the univariate OU. There is a vector $\vec{\theta}$ of long-run averages for $a_{S,opt}$ and $g_{s,opt}$; the random fluctuations and 'pull' toward $\vec{\theta}$ are determined by Σ and A matrices, respectively. There is an analytical solution for the stationary variance of the univariate OU ($\sigma^2/2\alpha$); we solved the stationary variance for the multivariate OU using numerical integration. See the Notes S3 for further details on parameters

Table 2 Macroevolutionary predictions of competing hypotheses for the scaling of stomatal size and density and comparisons with estimates from phylogenetic comparative analyses of 2408 species of forest vascular plants.

	Macroevolutionary stationarity among species		Trait variance ratios at stationarity			Scaling exponent at stationarity	
Hypothesis	Trait means	Trait (co)variance	V^*_{dS}/V^*_{aS}	V^*_{dS}/V^*_{gmax}	V^*_{aS}/V^*_{gmax}	SMA	OLS
H_1: Stomatal-area adaptation	Neutral plane (Eqn S37)	Neutral plane (Eqn S42)	4	∞	∞	0.5 (Eqn S43)	0.5 (Eqns S44, S45)
H_2: Stomatal-area minimization	Stable (Eqn S51)	Stable (Eqn S52)	1	4	4	1 (Eqn S53)	1 (Eqns S54, S55)
H_3: Stomatal adaptation + bounded size	Stable (Eqn S63)	Stable (Eqn S64)	Likely > 1	Likely > 1	Variable	Variable (Eqn S66)	Variable (Eqns S67, S68)
Estimates	See Table 3		1.26 [1.16–1.36]	1.27 [1.16–1.32]	1.01 [0.895–1.11]	0.523 [0.436–0.563] 2.42 [2.24–3.01]	1.12 [1.08–1.17]

The models differ in whether they predict the among-species means and (co)variance in stomatal density and size form a neutral plane or a stable point. The equation number in parentheses cross references the relevant part of the Supporting Information. We also compared the ratio of trait variances at stationarity, where V^*_{dS}, V^*_{aS}, and V^*_{gmax} are the stationary variances in stomatal density, size, and $g_{s,max}$ on log scales, respectively. These quantities can be deduced from the associated equations for the stationary variance. We compared these predictions to estimated values from vascular plants shown in the bottom row. The range in brackets indicated the 95% bootstrap confidence interval. Finally, we predict the scaling exponent that would be estimated using ordinary least-squares (OLS) and standardized major axis regression methods. The equation numbers in parentheses cross references the relevant part of the Supporting Information. For comparison, the estimates using each method on our data set are given in the bottom row. The OLS estimates differ depending on which variable is treated as the explanatory variable, stomatal density (upper) or stomatal size (lower). The range in brackets indicated the 95% bootstrap confidence interval.

and analysis. From the stationary distribution, we calculate the expected interspecific scaling exponent one would estimate regressing density against size using OLS or SMA methods on a random sample of species.

For all hypotheses, two key assumptions are that the fluctuations in the adaptive optima are sufficiently small, and the genetic variance is sufficiently large that every species closely tracks the fluctuating optima. This enables us to approximate the stationary distribution of species trait means using the stationary distribution of the adaptive optima. In Notes S3, we discuss the parameter space we analyzed in which this assumption would be met and confirmed the validity of the assumption using recursion simulations. An additional simplifying assumption is that the OU process is homogeneous among species and through time (i.e. there are no major discontinuities in the environment or between adaptive regimes *sensu*; Uyeda & Harmon 2014).

Stomatal trait data from global forests

The stomatal data set of global forests represents a total of 2408 plant species from natural forests (Fig. 2), including novel field data collected from Chinese forest communities and a compilation of published literature values. The data set includes representatives of all major vascular plant clades (angiosperms, gymnosperms, and pteridophytes) covering 201 families and 934 genera. For each species, we calculated $g_{s,max}$ and f_S, where f_S is proportional to the stomatal pore area index, which defined as the product of D_S and stomatal length (L) squared (Sack *et al.*, 2003), because $A_S = mL^2$ (Sack & Buckley, 2016).

We calculated $g_{s,max}$ (Eqn 2) to water vapor at a reference leaf temperature ($T_{leaf} = 25°C$) following Sack & Buckley (2016). They defined biophysical and morphological constants as:

$$b = \frac{D_{wv}}{v} \qquad \text{Eqn 8}$$

$$m = \frac{\pi c^2}{j^{0.5}(4hj + \pi c)} \qquad \text{Eqn 9}$$

b is the diffusion coefficient of water vapor in air (D_{wv}) divided by the kinematic viscosity of dry air (v). $D_{wv} = 2.49 \times 10^{-5}$ m^2 s^{-1} and $v = 2.24 \times 10^{-2}$ m^3 mol^{-1} at 25° (Monteith & Unsworth, 2013). For kidney-shaped guard cells, $c = h = j = 0.5$; for dumbbell-shaped guard cells in the Poaceae, $c = h = 0.5$ and $j = 0.125$. We used the species average $g_{s,max}$ and f_S for all analyses.

Phylogenetic comparative analyses

We implemented a multivariate phylogenetic comparative method to estimate scaling between stomatal density and size using the OU model. This provides an estimate of scaling as directly connected to our model predictions as possible. Our analysis revealed that neither OLS nor SMA regression, even when incorporating phylogenetic structure, would estimate an

Table 3 Phylogenetic comparative estimates of among species stomatal trait means and variances at stationarity.

	Macroevolutionary stationarity among species		
		Trait (co)variance	
	Trait mean	Parameter estimates	Implied macroevolutionary parameters
	Stomatal density	$\begin{bmatrix} \widehat{V}^*_{dS} & \\ \widehat{V}^*_{dS,aS} & \widehat{V}^*_{aS} \end{bmatrix} = \begin{bmatrix} 0.585 & \\ -0.242 & 0.465 \end{bmatrix}$	$\begin{bmatrix} \mathrm{Var}(a_{S,opt}) & \\ \mathrm{Cov}\left(a_{S,opt}, \log\left(g_{s,opt}\right)\right) & \mathrm{Var}\left(\log\left(g_{s,opt}\right)\right) \end{bmatrix} = \begin{bmatrix} 0.465 & \\ -0.011 & 0.458 \end{bmatrix}$
Angiosperms	174 [167–180] mm^{-2}	$\left(\begin{bmatrix} 0.547 & \\ -0.267 & 0.434 \end{bmatrix} - \begin{bmatrix} 0.633 & \\ -0.204 & 0.500 \end{bmatrix}\right)$	$\left(\begin{bmatrix} 0.434 & \\ -0.029 & 0.429 \end{bmatrix} - \begin{bmatrix} 0.500 & \\ 0.030 & 0.536 \end{bmatrix}\right)$
Gymnosperms	80.8 [62.3–105] mm^{-2}		
Pteridophytes	73.1 [63.4–85.7] mm^{-2}		
	Stomatal size		
Angiosperms	250 [243–257] μm^2		
Gymnosperms	677 [533–881] μm^2		
Pteridophytes	762 [665–865] μm^2		

The trait means are estimated separately for Angiosperms, Gymnosperms, and Pteridophytes on a log scale, but transformed to measurement units here. The range in brackets is the 95% bootstrap confidence interval. Note that stomatal size refers to the area of the entire stomatal complex (guard cells and pore), not the pore area. We estimated a single stationary trait covariance matrix for all groups. The matrices in brackets are the 95% bootstrap confidence intervals for each element of the matrix. V^*_{dS} and V^*_{aS} are the stationary variances for stomatal density and size, respectively, on a log scale; $V^*_{dS,aS}$ is the stationary covariance on a log scale. The implied macroevolutionary parameters are the stationary variance in optimal stomatal size ($\mathrm{Var}(a_{S,opt})$), optimal $g_{s,max}$ ($\mathrm{Var}(\log(g_{s,opt}))$), and their covariance ($\mathrm{Cov}(a_{S,opt}, \log(g_{s,opt}))$). See the Note S3 for explanation of implied macroevolutionary parameters.

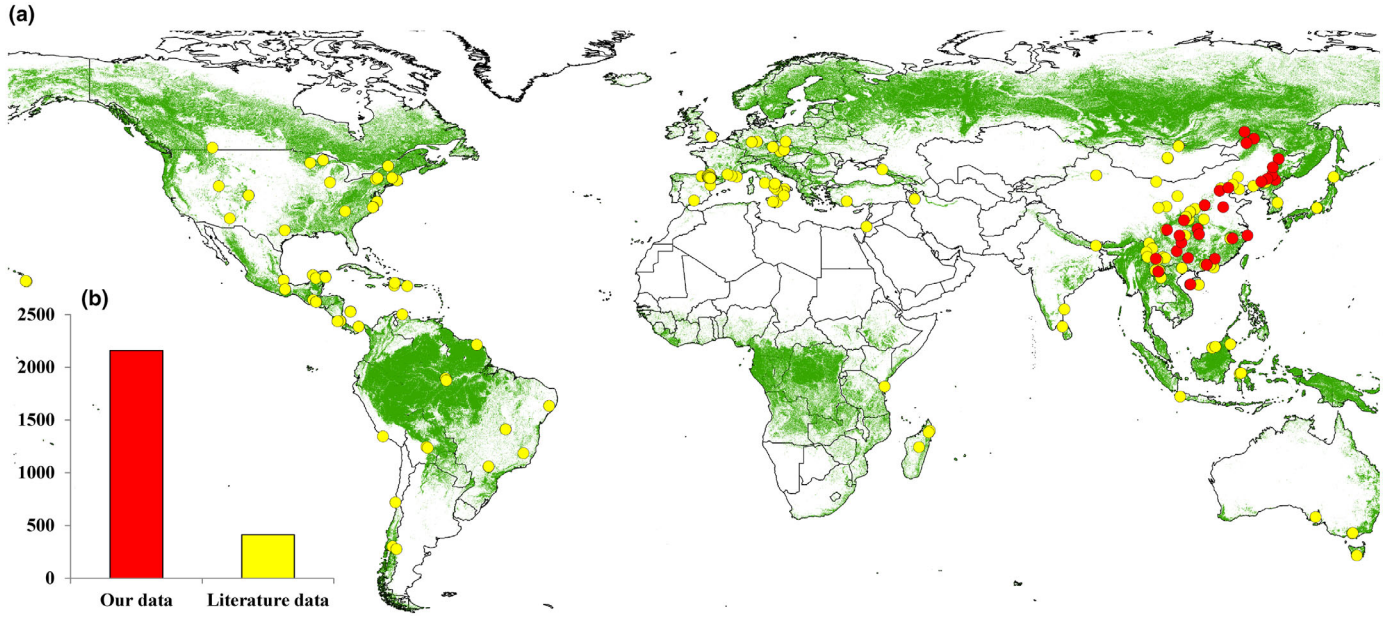

Fig. 2 Geographic distribution of sampling sites (a) and the number of plant species (b) in this study. Green areas indicate forested biomes.

interpretable scaling exponent when stomatal size is bounded (see the Results section). Therefore, we estimated the among-species covariance directly and report the expected OLS and SMA scaling exponent estimates if one regressed d_S on a_S (Eqns S16 and S17 in the Supporting Information). The choice of regressing d_S on a_S or vice versa is arbitrary in this case and is unrelated to a cause-and-effect relationship.

We used the Plant List (http://www.theplantlist.org) to confirm species names; then, we assembled a synthetic phylogeny using S.PhyloMaker (Qian & Jin, 2015). We estimated the parameters of the multivariate OU using the Ornstein–Uhlenbeck for Comparative Hypotheses (OUCH) model in the R package MVSLOUCH v.2.7.6 (Bartoszek *et al.*, 2012, 2024) and the phylogeny described above. To test for shifts in OU

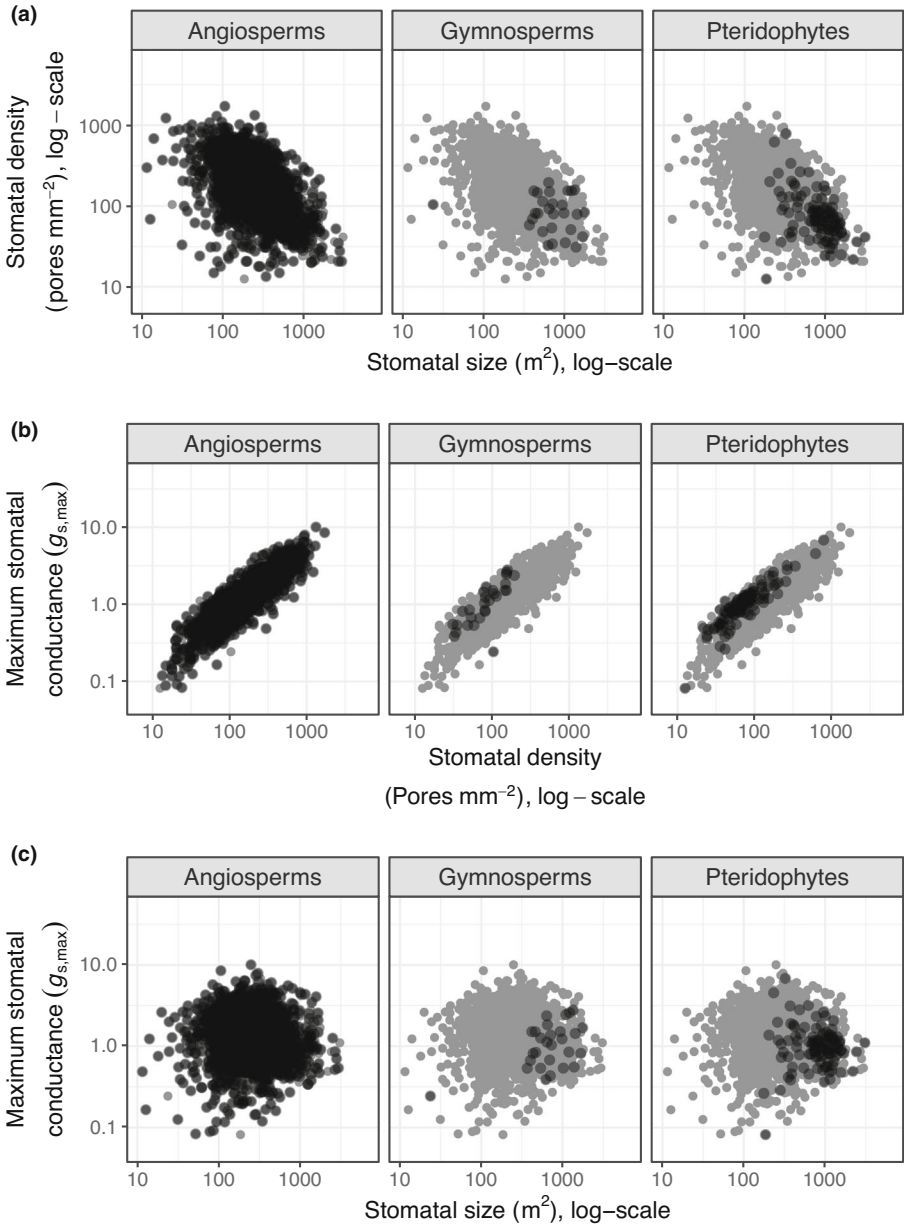

Fig. 3 Inverse stomatal size–density scaling across vascular land plants and its relationship with anatomical maximum stomatal conductance ($g_{s,max}$). In all panels, dark points represent species mean trait values from the focal group; gray background points are from all groups for comparison. The panels show the relationship between (a) stomatal size and density, (b) stomatal density and $g_{s,max}$, and (c) stomatal size and $g_{s,max}$ for the same global data set of forest plants. All panels are on a log–log scale.

parameters between major groups, we estimated separate mean trait values for Angiosperms, Pteridophytes, and Gymnosperms. From the estimated multivariate OU parameters, we calculated the bivariate normal stationary distribution. Using the stationary distribution is appropriate here because the phylogenetic half-life (see the Results section) is much shorter than the root of the phylogeny, meaning there is sufficient time for stationarity to have been reached. Our covariance estimates account for phylogenetic nonindependence because the OU parameters were estimated using the phylogeny. We estimated 95% confidence intervals for all parameters using 1000 parametric bootstrap samples generated by simulating from the best-fit model and refitting. One gymnosperm species, *Torreya fargesii* Franch. (Taxaceae), had substantially lower stomatal size than would be predicted from its density (Fig. 3a). The results of the paper did not change if this outlier was excluded. Therefore, we excluded this species from statistical analyses but show it in the figure for completeness. All data were analyzed in R v.4.4.2 (R Core Team, 2025).

Results

The expression of stomatal-area adaptation and minimization hypotheses in the mathematics of EQG provides specific quantitative predictions about the central tendencies and (co)variances of stomatal density and size, both within and among species. Table 1 summarizes the model predictions within species; Table 2 summarizes the model predictions among species and compares them to estimates from phylogenetic comparative analysis of vascular forest plants. Complete derivations are available in Notes S3. In this section, we do not exhaustively analyze all parameter space but rather focus on whether or under what

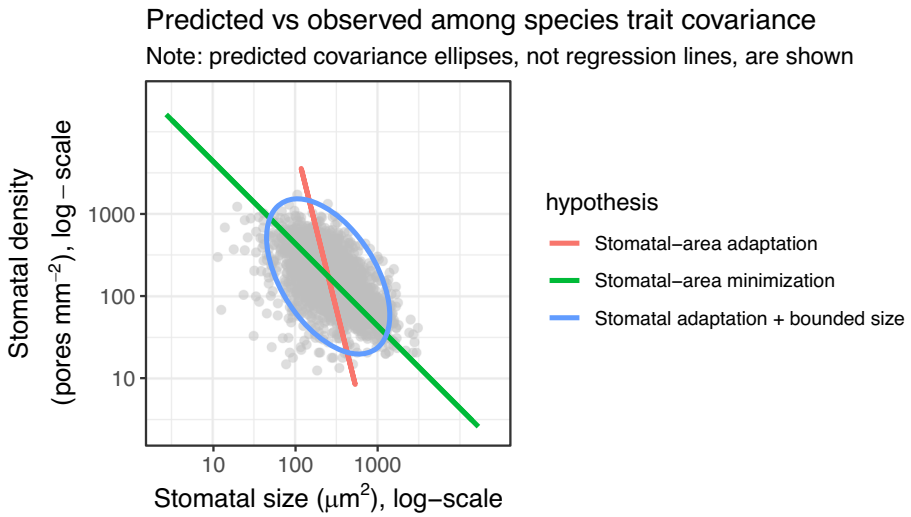

Fig. 4 The 'stomatal adaptation + bounded size' hypothesis, with tuning, predicts among species covariation in stomatal size and density, whereas simpler hypotheses do not. The gray points represent species mean trait values, as shown in Fig. 3. Colored polygons are 99% quantile ellipses predicted by each hypothesis, albeit tuned based on empirical constraints. The red and green ellipses appear as straight lines because these hypotheses incorrectly predict zero variance orthogonal to the main axis of variation. By contrast, the last hypothesis predicts significant variance orthogonal to the main axis of variation that is not due simply to measurement error, but real biological variation among species. For all hypotheses, the predicted ellipses are tuned to match estimated stationary trait means and variance in anatomical maximum stomatal conductance ($g_{s,max}$). The plot is on a log–log scale.

conditions the hypotheses make realistic predictions. After that, we compare these predictions to parameter estimates from a phylogenetic comparison of vascular forest plants.

Neither stomatal-area adaptation nor minimization hypotheses are inconsistent with observations

The stomatal-area adaptation hypothesis assumes that selection only optimizes $g_{s,max}$ and that the optimal $g_{s,max}$ fluctuates following a univariate OU process. Note that there are many other assumptions in the EQG model, but these are the assumptions that differentiate this hypothesis from the other hypotheses. Under this hypothesis, stomatal density and size evolve as a by-product of selection on $g_{s,max}$. Problems with the stomatal-area adaptation hypothesis arise because there are no bounds on stomatal size. This results in infinite genetic variance in both stomatal density and size despite a well-defined genetic correlation between them (Table 1). Even if we assume finite genetic variance within species, the among-species distribution reaches a stable covariance structure, but it is not stationary. Hence, the hypothesis makes precise, testable predictions about SMA and OLS slopes (Table 2), but cannot be sufficient because it predicts infinite variances.

The stomatal-area minimization hypothesis adds directional selection for decreased f_S along with stabilizing selection on $g_{s,max}$. Therefore, this hypothesis constrains the within- and among-species variances to be finite (Tables 1, 2), but its predictions about interspecific scaling are inconsistent with the data. Specifically, this model predicts zero variance in f_S among species (Eqn S51 in the Supporting Information), which is inconsistent with observations (Fig. S1). Consequently, the hypothesis predicts much greater variance in a_S and d_S relative to $g_{s,max}$ compared with observations (Table 2). It also predicts a complete negative correlation between size and density among species (Fig. 4). These inconsistencies between predictions and observations arise because there are no bounds on how small or large stomata can be, an assumption that is not supported by our understanding of stomatal function in real leaves (see the Discussion section).

The stomatal adaptation + bounded size hypothesis makes predictions consistent with observations

The inconsistencies between the previous two hypotheses and data forced us to modify them by making the additional, albeit realistic, assumption that stomatal dimensions are bounded by selection against extremely large or small pore size. We analyzed two versions of this hypothesis. The simpler version of this hypothesis assumed constant optimal stomatal size, $a_{S,opt}$. This simpler version predicts variance in d_S, $g_{s,max}$, and f_S, but no variance in a_S, as noted previously in the Materials and Methods section. This is inconsistent with the wide variation in stomatal size and implies that $a_{S,opt}$ must be a variable, not a constant. In other words, optimal stomatal size varies, presumably depending on the environment and other traits of a species. Although we did not explicitly model exogenous factors that would explain variation in $a_{S,opt}$, we review mechanistic hypotheses in the Discussion section. With the assumption that $a_{S,opt}$ fluctuates according to an OU process, the model can predict realistic within-species patterns of trait means and covariances (Table 1), finite and realistic variances among species, and inverse size–density scaling (Table 2; Fig. 4). Importantly, the hypothesis is internally consistent in that the parameter values necessary to obtain realistic predictions are similar to those estimated using phylogenetic comparative methods (will be discussed later). The problem with this

hypothesis is that its predictions cannot be derived from first principles and must be tuned by parameter estimates from the data it is meant to explain. Therefore, the fact that the model predicts trait (co)variance that matches the observation (Fig. 4) does not necessarily indicate strong support for the hypothesis because it could be an artifact of tuning the parameters to match the data. To better test how well the hypothesis predicts trait (co)variance, we need an independent way to either predict from first principles or estimate the limits on optimal $g_{s,max}$, f_S, and a_S in vascular land plants.

Genetic covariance within species

Under the stomatal-area adaptation hypothesis, the genetic variance increased without bound to a stable covariance structure (Eqn S34) in which stomatal density and size were perfectly negatively correlated. The other hypotheses resulted in finite genetic (co)variance matrices (Table 1) that we solved for numerically over a range of parameter space. The equilibrium genetic variance increases as mutational variance increases and the strength of selection on $g_{s,max}$ decreases (Figs S2, S3). Similarly, stronger selection to minimize f_S (Fig. S4) or optimize stomatal size (Fig. S5) reduces genetic variance. Under the stomatal-area minimization hypothesis, the genetic correlation between traits is always negative (Fig. S6), whereas under the stomatal adaptation + bounded size hypothesis, the correlation can be positive if the mutational correlation is sufficiently positive (Fig. S7).

Microevolutionary responses to selection can be decoupled from macroevolutionary patterns

In EQG, the short-term (single generation) response to multivariate selection is determined by the additive genetic (co)variance between traits and the selection gradient (Lande, 1979). The additive genetic (co)variance at equilibrium is determined by the mutational variance and the curvature of the fitness surface. There is no mathematically necessary relationship between the genetic variance, the selection gradient, and the long-term macroevolutionary movement of adaptive optima. Indeed, our models predict these factors are generally decoupled from one another for stomatal size and density except under special cases and coincidental areas of parameter space. This is evident by the fact that the genetic (co)variance matrix does not appear in the equations for the equilibrium among-species (co)variance except the stomatal-area adaptation hypothesis (compare sections S3.3.1.6 to S3.3.2.6 and S3.3.3.6 in the Supporting Information).

The stomatal-area adaptation hypothesis is one special case in which the genetic variance, response to selection, and among-species covariance are aligned. It predicts a very specific negative genetic (co)variance structure (Table 1) that is insensitive to the mutational variance. It also predicts that the response to selection on $g_{s,max}$ always results in opposing response directions for stomatal density and size (Figs S8–S10). Both the genetic (co)variance and response to selection are aligned with the among-species (co)variance (Table 1). For the other two hypotheses, there are few generalizations. For example, the stomatal-area minimization hypothesis predicts a greater response in stomatal density relative to size, but the covariance of the response is sensitive to the genetic covariance (Fig. S8). Furthermore, size can respond more strongly if it has greater genetic variance (Fig. S9). Under the stomatal adaptation + bounded size hypothesis, stomatal size tends to respond more strongly to selection on $g_{s,max}$ than density, but both generally respond in a coordinated manner under most parameter space (Figs S8, S9). As selection to minimize f_S strengthens, stomatal size responds more strongly than density because this allows leaves to increase $g_{s,max}$ without increasing f_S as much (Fig. S10).

Except in special cases, these short-term responses to selection on $g_{s,max}$ do not predict the interspecific (co)variance in stomatal density and size. This is because the mean trait values at *equilibrium* in a species do not necessarily depend on the specific short-term dynamics. We assumed sufficiently large population sizes and mutational variance relative to fluctuations in the adaptive optimum that all species could closely track their fitness optima. These assumptions will not always be met in nature, but this adaptive tracking model best fits observations for many traits in many species. With that assumption, we derived expected stationary distributions of stomatal trait values among species, and these equations do not include any microevolutionary parameters (Table 2). Simulations described in Notes S4 showed this approximation is valid over a wide range of variation in mutation (Fig. S11), mutational correlation (Fig. S12), and strengths of selection on $g_{s,max}$ (Fig. S13), f_S (Fig. S14), and a_S (Fig. S15).

Phylogenetic comparative estimates of stomatal trait variation among species

We estimated stomatal size–density scaling in 2408 forest plant species from new field-collected samples over 28 sites in China and global synthesis of data from the literature (Fig. 2). Stomatal density was lower and size was higher in gymnosperms and pteridophytes than in angiosperms (Table 3). Among all groups, stomatal density varies more than size, and there is strong negative covariance (Table 3; Fig. 3). As mentioned previously, the interspecific trait variance is inconsistent with either the stomatal-area adaptation or minimization hypotheses. The stomatal-area adaptation hypothesis predicts that the SMA and OLS estimates of the scaling exponent should be close to 0.5 and the variance of a_S and d_S should be much greater than that of $g_{s,max}$ (Table 2). The OLS estimate was close to 0.5 only when size is used as the explanatory variable, but the other predictions were not supported. The stomatal-area minimization hypothesis predicts that SMA and OLS estimates of the scaling exponent should be close to unity and the variance of a_S and d_S should be similar and 4× greater than the variance in $\log(g_{s,max})$ (Table 2). The SMA estimate was close to unity, similar to the results of de Boer *et al.* (2016), but the other predictions were not supported. The stomatal adaptation + bounded size hypothesis predicts among species trait (co)variances that are quantitatively consistent with the data as well as within species trait (co)variances that are qualitatively plausible. Based on the stationary trait distribution (Eqn S64), the phylogenetic

estimates of V^*_{dS}, V^*_{aS}, and V^*_{dSaS} (Table 2) imply essentially zero covariance between $a_{s,opt}$ and $g_{s,opt}$ (Eqn S65; Table 3). In other words, the among-species scaling we observe implies that the ecological conditions that favor high $g_{s,max}$ are decoupled from those that favor small or large stomata.

Discussion

Ours is the first attempt to derive predictions about scaling between stomatal density and size from fundamental evolutionary theory and biophysical models of diffusion. This is an important advance for two reasons. First, any evolutionary explanation needs to be consistent with laws of inheritance and evolutionary forces of selection, drift, and mutation. Second, these models provide specific quantitative predictions that can be compared with data. By comparing our predictions to a data set of mean stomatal density and size from 2408 vascular forest plant species using phylogenetic comparative methods, we arrive at three main conclusions. First, neither selection to optimize anatomical maximum conductance ($g_{s,max}$) nor selection to minimize epidermal area allocated to stomata (f_S) can adequately explain the covariance between stomatal density and size. We therefore posit that additional selection to optimize stomatal size within bounds is probably required to account for the limited variance in this trait. Second, there is no necessary relationship between within- and among-species size–density scaling. Many patterns of genetic variation result in the same interspecific pattern. When species have large enough populations and enough genetic variance to track fluctuations in adaptive optima, trait variation is controlled in a top-down manner by the macroevolutionary adaptive landscape. Third, when stomatal size is bounded, neither SMA nor OLS methods estimate scaling exponents between stomatal density and size that are interpretable without further information. Researchers should therefore make use of the full covariance structure and independent predictions to evaluate competing hypotheses. We discuss the implications of our study, its limitations, and advice for future research later.

We identified two distinct hypotheses for inverse stomatal size–density scaling that we label 'stomatal-area adaptation' and '-stomatal-area minimization' hypotheses. We are not the first to describe these hypotheses, but the labels and associated fitness functions clarify key assumptions and testable predictions. Under the stomatal-area adaptation hypothesis, selection only optimizes $g_{s,max}$ (Eqn 5), meaning that f_S will increase when selection favors greater $g_{s,max}$, and vice versa for selection to lower $g_{s,max}$. Inverse size–density scaling emerges because there is an ellipse in density-size space for a given amount of variation in $g_{s,max}$, either within or among species. However, the size of this ellipse is unstable. Variance in density and size grows unchecked, and their covariance becomes negative because of limited variance in $g_{s,opt}$. This model clearly shows that additional bounds on stomatal traits must be acting in nature. The stomatal-area minimization hypothesis adds a constraint on f_S, favoring changes in $g_{s,max}$ that minimize increases in f_S (Eqn 6). The $g_{s,max}$ and f_S can evolve semi-independently because of differential scaling and apparent constraint on guard cell shape (see the Introduction section). This assumption stabilizes the variance in stomatal density and size within (Table 1) and among (Table 2) species. Despite our different theoretical approaches, our derivation mirrors the conclusion from de Boer *et al.* (2016) that selection to minimize f_S shapes how size and density diverge to achieve lower and higher $g_{s,max}$. However, our analysis reveals that under this hypothesis, stomatal density and size should be much more variable among species than $g_{s,max}$, a prediction that is not supported by the data (Table 2; Fig. 4). This led us to hypothesize that bounds on stomatal size limit the variance in density and size among species, which we refer to as the 'stomatal adaptation + bounded size' hypothesis. Our analysis shows that when optimal stomatal size varies, this hypothesis makes predictions that are consistent with observations in certain areas of parameter space. We discuss this further later in our analysis of macroevolutionary parameters in forest plants. Thus, our analysis reconciles two previous hypotheses by showing that both selection on optimal $g_{s,max}$ and selection to minimize f_S may be necessary, but not sufficient to explain inverse size–density scaling. Below, we discuss directions for future research on the adaptive significance of stomatal size, which could better resolve the forces shaping covariance between stomatal traits within and among species.

When the trait variance is finite ('stomatal-area minimization' and 'stomatal adaptation + bounded size' hypotheses), the genetic covariance within species does not affect the long-term pattern of interspecific trait covariance. This is not necessarily surprising because it has long been known that genetic covariance can have minimal impact on long-term phenotypic evolution. At equilibrium, the genetic (co)variance matrix is determined by the mutational (co)variance, strength of selection, and other model parameters that affect the shape of the adaptive landscape (Figs S2–S7). However, when there is sufficient genetic variation in the direction of selection, trait values will reach their adaptive optima (Figs S11–S15). In general, the genetic covariance can bias evolutionary trajectories when there are multiple adaptive optima by pushing the population to an optimum in the direction of greater genetic variance. However, in our model, fitness landscapes were smooth and did not provide an opportunity for genetic covariance to alter long-term evolution in this way. One implication of this result is that intra- and interspecific scaling between stomatal density and size will not necessarily be the same and/or have the same underlying cause. The observation that stomatal density and size usually negatively covary within (Wilson, 1972; Ciha & Brun, 1975; Franks *et al.*, 2009; Xie *et al.*, 2021) and among species (Weiss, 1865; Franks & Beerling, 2009b; de Boer *et al.*, 2016; Sack & Buckley, 2016; Liu *et al.*, 2023) mirrors many other cases of correspondence between scales (Tsuboi *et al.*, 2024) and deserves further research. A second implication is that we can use the stationary distribution of adaptive optima to accurately approximate the among species (co)variance in stomatal density and size. The remaining discussion focuses on predictions regarding interspecific variance using this approach.

In comparative ecology, it is commonly assumed that when trait–trait relationships are governed by equations with the form

shown in Eqns 1 and 2, scaling relationships can be estimated using regression methods, typically SMA or OLS. Our evolutionary analysis reveals that this assumption holds when trait variance is unconstrained but breaks down if there are additional bounds on trait variance (Table 2). In this case, bounds and selection in stomatal size alter the covariance with stomatal density. With stabilizing selection on size, stomatal density is relatively less constrained in responding to selection, resulting in a weaker association between size and density than would otherwise occur. We visualized this by plotting the among-species covariance ellipses predicted at stationarity by different hypotheses but constrained by empirical estimates of the mean trait values and variance in $g_{s,max}$ (Fig. 4). The simpler hypotheses predict highly constrained trait covariance along a single axis of variation, whereas the stomatal adaptation + bounded size hypothesis accommodates the variation orthogonal to the main axis of variation. Even if the simpler hypotheses were correct, empirical data sets would be variable because of measurement error. However, the biological variation in our very broad survey of forest plants is large relative to measurement error. Uncovering the evolutionary forces that gave rise to stomatal anatomical diversity among vascular forest plants cannot be determined from bivariate slopes alone. Instead, we recommend analyzing the entire (co)variance within and among species and estimating key micro- and macroevolutionary parameters that can inform the relative importance of selection $g_{s,max}$, f_S, and stomatal size (Tables 1, 2).

Since our model demonstrates that interspecific scaling alone cannot uniquely identify which selective processes shape stomatal size and density, we considered the entire covariance structure in a phylogenetic comparative framework. Under the stomatal adaptation + bounded size hypothesis, fluctuating selection on $g_{s,max}$ and a_S, along with selection to minimize f_S, determines a unique covariance among stomatal density and size (Eqn S64). These predictions enable a novel interpretation of the estimated covariance in stomatal density and size (Table 3). Specifically, the covariance pattern is consistent with independently fluctuating optimal $g_{s,max}$ and a_S (the range of implied covariances overlaps zero, Table 3). This interpretation makes sense of three observations that would not otherwise be obvious. First, it explains why stomatal density varies more than stomatal size among species under most areas of parameter space. The hypothesis also explains two related observations – d_S and $g_{s,max}$ positively covary (Fig. 3b), whereas a_S and $g_{s,max}$ covary little within major groups (Fig. 3c). Based on Eqn 2, a naïve null model might predict similar variance in a_S and d_S and positive covariance between both a_S and d_S with $g_{s,max}$. However, when the adaptive optima for a_S and $g_{s,max}$ fluctuate independently and species track those optima, our model predicts no covariance between a_S and $g_{s,max}$ at stationarity. This results in greater variance in d_S and stronger positive covariance between d_S and $g_{s,max}$ because d_S is less constrained to respond to selection on $g_{s,max}$. Within species, a_S often cannot respond as much to selection on $g_{s,max}$ because if a_S deviates far from $a_{S,opt}$, fitness will decline; d_S is relatively free to respond since it only indirectly affects fitness through its effect on $g_{s,max}$. At a macroevolutionary scale, this results in greater variance (less constraint) in d_S and positive covariance between d_S and $g_{s,max}$. It might seem counterintuitive that the optima for a_S and $g_{s,max}$ fluctuate independently since small stomata are necessary to achieve the greatest observed $g_{s,max}$ (Franks & Beerling, 2009a,b). The shift toward higher stomatal density and smaller size in Angiosperms (Table 3), whatever its ultimate cause (e.g. genome downsizing), contributes to this pattern. But our analysis shows that loosening the lower bounds on guard cell size simultaneously increases the variance in a_S and makes the covariance with d_S more negative (Eqn S64). Thus, changing constraints on stomatal size can open space for leaves with high $g_{s,max}$ and small stomata even when they evolve independently.

A major implication of our models is that bounds on stomatal size and fluctuating selection on optimal stomatal size within these bounds play an important role in shaping the size–density scaling relationship. Minimum guard cell size is a function of genome size and its scaling relationships with nuclear and primordial cell size (Beaulieu *et al.*, 2008; Šímová & Herben, 2012; Roddy *et al.*, 2020). An alternative hypothesis is that extremely small stomata are deleterious because they inhibit gas exchange when collisions with guard cell walls dominate the diffusion (Hodgson *et al.*, 2010). This effect becomes important and reduces stomatal conductance when pore width approaches 0.5–1 μm (Csiro, 1983). Hence, in plant species with large genomes, guard cell size may set the minimum stomatal pore length, whereas in species with small genomes, selection against extremely small pores may set the minimum stomatal size. On the other extreme, large guard cells are likely deleterious because the lower surface area to volume ratio of larger cells slows the rate of stomatal closure (Drake *et al.*, 2013; Raven, 2014), all else being equal. Plants can partially compensate for guard cell geometry by increasing the rate of transport per unit surface area (Lawson & Blatt, 2014), but this would likely involve costs such as constructing and maintaining transporter proteins. In summary, it is near certain that factors such as genome size, diffusion, and guard cell mechanics set bounds on stomatal size independent of the effect on $g_{s,max}$.

Within these overall bounds on guard cell size, stomatal size per se is likely under selection independent of its effect on $g_{s,max}$, but the adaptive significance of variation in stomatal size is not well understood. One hypothesis is that smaller guard cells close and open faster in response to environmental stimuli because of their greater surface area to volume ratio (Drake *et al.*, 2013), as discussed in the previous paragraph. Faster responses allow leaves to closely track variable light, humidity, and other factors, keeping stomatal conductance closer to its short-term optimum. All else being equal, faster response increases water-use efficiency for a given operational stomatal conductance (Drake *et al.*, 2013; Lawson & Vialet-Chabrand, 2019). Smaller stomata respond faster to environmental change within groups of closely related species (Drake *et al.*, 2013; Yoshiyama *et al.*, 2024), but size is less predictive of speed in broader taxonomic comparisons (Elliott-Kingston *et al.*, 2016; McAusland *et al.*, 2016; Haworth *et al.*, 2018). These observations suggest that the speed of stomatal response is modulated by factors other than guard cell size, such as the rate of membrane transport and mechanical advantage of adjacent epidermal cells (Lawson & Blatt, 2014). This hypothesis predicts that selection for faster stomatal response would

result in smaller stomata over short or moderate evolutionary timescales. Consistent with those predictions, smaller stomata are associated with greater water-use efficiency in more arid populations of *Arabidopsis* (Dittberner *et al.*, 2018) and *Populus trichocarpa* (Klein *et al.*, 2025). However, it is unclear what the cost of small stomata is and, hence, why selection would favor larger stomata, holding $g_{s,max}$ constant. Faster response in small guard cells may be more energetically demanding (Raven, 2014) and therefore selected against in more predictable and/or less variable environments. However, this hypothesis has not been tested to our knowledge. Despite incomplete understanding of how selection operates on stomatal size, associations between stomatal size and environment within and among species indicate that this trait is under selection independent of its effects on $g_{s,max}$.

Conclusion

We addressed the long-standing observation of inverse stomatal size–density scaling among plant species by considering evolutionary hypotheses based on optimizing maximum stomatal conductance ($g_{s,max}$) and minimizing epidermal surface area allocated to stomata (f_S). Considering only these factors predicts more variance in size and density relative to $g_{s,max}$ than we observe in a global data set of forest plants. Selection and bounds on stomatal size reduce variation in both size and density relative to $g_{s,max}$. If selection on $g_{s,max}$ and stomatal size fluctuates independently, this can explain both inverse size–density scaling and the strong positive covariance between $g_{s,max}$ and f_S. The estimated scaling exponents using common statistical methods are sensitive to bounds on stomatal size and therefore future research testing these hypotheses should complement interspecific comparative studies with quantitative genetic and phenotypic selection approaches.

Acknowledgements

Peter Franks, Ben Blonder, three anonymous reviewers, Kate McCulloh, and members of her lab provided constructive feedback on a previous version of this manuscript. Financial support was provided by the National Natural Science Foundation of China (32588202, 32430067, 32201311), the National Key R&D Program of China (2022YFF080210102), the US National Science Foundation 1929167 (to CDM), and the Key Laboratory of Ecology and Environment in Minority Areas (Minzu University of China), National Ethnic Affairs Commission (KLEEMA20230), the 10th Young Elite Scientists Sponsorship Program by CAST, and the Academic Team Leadership Program Project of Minzu University of China (2024XSYL01).

Competing interests

None declared.

Author contributions

NH and GY designed field sampling. CDM, LS, NH, CL and HJB conceived the initial ideas. CL, NH, YL, JZ, ZZ, ML and LX collected the data; CL wrote the first draft, and CDM contributed the final mathematical derivations, data analysis and wrote the final manuscript. LS, HJB, CL, NH, GY and XH revised the manuscript. All authors gave final approval for publication. CL and CDM contributed equally to this work.

ORCID

Hugo Jan de Boer https://orcid.org/0000-0002-6933-344X
Nianpeng He https://orcid.org/0000-0002-0458-5953
Congcong Liu https://orcid.org/0000-0003-3949-4194
Christopher D. Muir https://orcid.org/0000-0003-2555-3878
Lawren Sack https://orcid.org/0000-0002-7009-7202

Data availability

The raw data and R code supporting the findings of this study are openly available in Zenodo at doi: 10.5281/zenodo.17155106.

References

Arnold SJ, Pfrender ME, Jones AG. 2001. The adaptive landscape as a conceptual bridge between micro- and macroevolution. *Genetica* **112**: 9–32.

Baird AS, Medeiros CD, Caringella MA, Bowers J, Hii M, Liang J, Matsuda J, Pisipati K, Pohl C, Simon B *et al.* 2024. How and why do species break a developmental trade-off? Elucidating the association of trichomes and stomata across species. *American Journal of Botany* **111**: e16328.

Baresch A, Crifò C, Boyce CK. 2019. Competition for epidermal space in the evolution of leaves with high physiological rates. *New Phytologist* **221**: 628–639.

Bartoszek K, Pienaar J, Mostad P, Andersson S, Hansen TF. 2012. A phylogenetic comparative method for studying multivariate adaptation. *Journal of Theoretical Biology* **314**: 204–215.

Bartoszek K, Tredgett Clarke J, Fuentes-González J, Mitov V, Pienaar J, Piwczyński M, Puchałka R, Spalik K, Voje KL. 2024. Fast MVSLOUCH: multivariate Ornstein–Uhlenbeck-based models of trait evolution on large phylogenies. *Methods in Ecology and Evolution* **15**: 1507–1515.

Beaulieu JM, Leitch IJ, Patel S, Pendharkar A, Knight CA. 2008. Genome size is a strong predictor of cell size and stomatal density in angiosperms. *New Phytologist* **179**: 975–986.

Berry JA, Beerling DJ, Franks PJ. 2010. Stomata: key players in the earth system, past and present. *Current Opinion in Plant Biology* **13**: 232–239.

de Boer HJ, Price CA, Wagner-Cremer F, Dekker SC, Franks PJ, Veneklaas EJ. 2016. Optimal allocation of leaf epidermal area for gas exchange. *New Phytologist* **210**: 1219–1228.

Brown HT, Escombe F. 1901. Static diffusion of gases and liquids in relation to the assimilation of carbon and translocation in plants. *Proceedings of the Royal Society of London* **67**: 124–128.

Ciha AJ, Brun WA. 1975. Stomatal size and frequency in soybeans. *Crop Science* **15**: 309–313.

Conesa MÀ, Muir CD, Molins A, Galmés J. 2019. Stomatal anatomy coordinates leaf size with Rubisco kinetics in the Balearic *Limonium*. *AoB Plants* **12**: 259.

Cornelissen JHC, Cerabolini B, Castro-Díez P, Villar-Salvador P, Montserrat-Martí G, Puyravaud JP, Maestro M, Werger MJA, Aerts R. 2003. Functional traits of woody plants: correspondence of species rankings between field adults and laboratory-grown seedlings? *Journal of Vegetation Science* **14**: 311–322.

Cramer W, Bondeau A, Woodward FI, Prentice IC, Betts RA, Brovkin V, Cox PM, Fisher V, Foley JA, Friend AD *et al.* 2001. Global response of terrestrial

ecosystem structure and function to CO_2 and climate change: results from six dynamic global vegetation models. *Global Change Biology* **7**: 357–373.

Csiro RL. 1983. Transport of gases into leaves. *Plant, Cell & Environment* **6**: 181–194.

Díaz S, Kattge J, Cornelissen JHC, Wright IJ, Lavorel S, Dray S, Reu B, Kleyer M, Wirth C, Colin Prentice I *et al.* 2016. The global spectrum of plant form and function. *Nature* **529**: 167–171.

Dittberner H, Korte A, Mettler-Altmann T, Weber APM, Monroe G, de Meaux J. 2018. Natural variation in stomata size contributes to the local adaptation of water-use efficiency in *Arabidopsis thaliana*. *Molecular Ecology* **27**: 4052–4065.

Dow GJ, Berry JA, Bergmann DC. 2014. The physiological importance of developmental mechanisms that enforce proper stomatal spacing in *Arabidopsis thaliana*. *New Phytologist* **201**: 1205–1217.

Drake PL, Froend RH, Franks PJ. 2013. Smaller, faster stomata: scaling of stomatal size, rate of response, and stomatal conductance. *Journal of Experimental Botany* **64**: 495–505.

Dunbar-Co S, Sporck MJ, Sack L. 2009. Leaf trait diversification and design in seven rare taxa of the *Hawaiian plantago* radiation. *International Journal of Plant Sciences* **170**: 61–75.

Elliott-Kingston C, Haworth M, Yearsley JM, Batke SP, Lawson T, McElwain JC. 2016. Does size matter? Atmospheric CO_2 may be a stronger driver of stomatal closing rate than stomatal size in taxa that diversified under low CO_2. *Frontiers in Plant Science* **7**: 1253.

Franks PJ, Adams MA, Amthor JS, Barbour MM, Berry JA, Ellsworth DS, Farquhar GD, Ghannoum O, Lloyd J, McDowell N *et al.* 2013. Sensitivity of plants to changing atmospheric CO_2 concentration: from the geological past to the next century. *New Phytologist* **197**: 1077–1094.

Franks PJ, Beerling DJ. 2009a. CO_2-forced evolution of plant gas exchange capacity and water-use efficiency over the Phanerozoic. *Geobiology* **7**: 227–236.

Franks PJ, Beerling DJ. 2009b. Maximum leaf conductance driven by CO_2 effects on stomatal size and density over geologic time. *Proceedings of the National Academy of Sciences, USA* **106**: 10343–10347.

Franks PJ, Drake PL, Beerling DJ. 2009. Plasticity in maximum stomatal conductance constrained by negative correlation between stomatal size and density: an analysis using *Eucalyptus globulus*. *Plant, Cell & Environment* **32**: 1737–1748.

Franks PJ, Farquhar GD. 2001. The effect of exogenous abscisic acid on stomatal development, stomatal mechanics, and leaf gas exchange in *Tradescantia virginiana*. *Plant Physiology* **125**: 935–942.

Freschet GT, Valverde-Barrantes OJ, Tucker CM, Craine JM, McCormack ML, Violle C, Fort F, Blackwood CB, Urban-Mead KR, Iversen CM *et al.* 2017. Climate, soil and plant functional types as drivers of global fine-root trait variation. *Journal of Ecology* **105**: 1182–1196.

Haworth M, Elliott-Kingston C, McElwain JC. 2011. Stomatal control as a driver of plant evolution. *Journal of Experimental Botany* **62**: 2419–2423.

Haworth M, Elliott-Kingston C, McElwain JC. 2013. Co-ordination of physiological and morphological responses of stomata to elevated [CO_2] in vascular plants. *Oecologia* **171**: 71–82.

Haworth M, Marino G, Materassi A, Raschi A, Scutt CP, Centritto M. 2023. The functional significance of the stomatal size to density relationship: interaction with atmospheric [CO_2] and role in plant physiological behaviour. *Science of the Total Environment* **863**: 160908.

Haworth M, Scutt CP, Douthe C, Marino G, Gomes MTG, Loreto F, Flexas J, Centritto M. 2018. Allocation of the epidermis to stomata relates to stomatal physiological control: stomatal factors involved in the evolutionary diversification of the angiosperms and development of amphistomaty. *Environmental and Experimental Botany* **151**: 55–63.

Hetherington AM, Woodward FI. 2003. The role of stomata in sensing and driving environmental change. *Nature* **424**: 901–908.

Hodgson JG, Sharafi M, Jalili A, Díaz S, Montserrat-Martí G, Palmer C, Cerabolini B, Pierce S, Hamzehee B, Asri Y *et al.* 2010. Stomatal vs. genome size in angiosperms: the somatic tail wagging the genomic dog? *Annals of Botany* **105**: 573–584.

Jordan GJ, Carpenter RJ, Koutoulis A, Price A, Brodribb TJ. 2015. Environmental adaptation in stomatal size independent of the effects of genome size. *New Phytologist* **205**: 608–617.

Klein MC, Meng Z, Bailey-Bale J, Milner S, Shi P, Muchero W, Chen J-G, Tschaplinski TJ, Jacobson D, Lagergren J *et al.* 2025. Climate adaptation in *Populus trichocarpa*: key adaptive loci identified for stomata and leaf traits. *New Phytologist* **247**: 2647–2664.

Lande R. 1979. Quantitative genetic analysis of multivariate evolution, applied to brain: body size allometry. *Evolution* **33**: 402–416.

Lawson T, Blatt MR. 2014. Stomatal size, speed, and responsiveness impact on photosynthesis and water use efficiency. *Plant Physiology* **164**: 1556–1570.

Lawson T, Vialet-Chabrand S. 2019. Speedy stomata, photosynthesis and plant water use efficiency. *New Phytologist* **221**: 93–98.

Lehmann P, Or D. 2015. Effects of stomata clustering on leaf gas exchange. *New Phytologist* **207**: 1015–1025.

Liu C, Sack L, Li Y, He N. 2022. Contrasting adaptation and optimization of stomatal traits across communities at continental scale. *Journal of Experimental Botany* **73**: 6405–6416.

Liu C, Sack L, Li Y, Zhang J, Yu K, Zhang Q, He N, Yu G. 2023. Relationships of stomatal morphology to the environment across plant communities. *Nature Communications* **14**: 6629.

Lundgren MR, Mathers A, Baillie AL, Dunn J, Wilson MJ, Hunt L, Pajor R, Fradera-Soler M, Rolfe S, Osborne CP *et al.* 2019. Mesophyll porosity is modulated by the presence of functional stomata. *Nature Communications* **10**: 2825.

McAusland L, Vialet-Chabrand S, Davey P, Baker NR, Brendel O, Lawson T. 2016. Effects of kinetics of light-induced stomatal responses on photosynthesis and water-use efficiency. *New Phytologist* **211**: 1209–1220.

McElwain JC, Steinthorsdottir M. 2017. Paleoecology, ploidy, paleoatmospheric composition, and developmental biology: a review of the multiple uses of fossil stomata. *Plant Physiology* **174**: 650–664.

McElwain JC, Yiotis C, Lawson T. 2016. Using modern plant trait relationships between observed and theoretical maximum stomatal conductance and vein density to examine patterns of plant macroevolution. *New Phytologist* **209**: 94–103.

Monteith JL, Unsworth MH. 2013. Chapter 2 – properties of gases and liquids. In: Monteith JL, Unsworth MH, eds. *Principles of environmental physics, 4th edn.* Boston, MA, USA: Academic Press, 5–23.

Muir CD. 2020. A stomatal model of anatomical tradeoffs between gas exchange and pathogen colonization. *Frontiers in Plant Science* **11**: 518891.

Murray M, Soh WK, Yiotis C, Spicer RA, Lawson T, McElwain JC. 2020. Consistent relationship between field-measured stomatal conductance and theoretical maximum stomatal conductance in C_3 woody angiosperms in four major biomes. *International Journal of Plant Sciences* **181**: 142–154.

Ordoñez JC, Van Bodegom PM, Witte J-PM, Wright IJ, Reich PB, Aerts R. 2009. A global study of relationships between leaf traits, climate and soil measures of nutrient fertility. *Global Ecology and Biogeography* **18**: 137–149.

Parlange J-Y, Waggoner PE. 1970. Stomatal dimensions and resistance to diffusion. *Plant Physiology* **46**: 337–342.

Qian H, Jin Y. 2015. An updated megaphylogeny of plants, a tool for generating plant phylogenies and an analysis of phylogenetic community structure. *Journal of Plant Ecology* **9**: 233–239.

R Core Team. 2025. *R: a language and environment for statistical computing.* Vienna, Austria: R Foundation for Statistical Computing.

Raven JA. 2014. Speedy small stomata? *Journal of Experimental Botany* **65**: 1415–1424.

Roddy AB, Théroux-Rancourt G, Abbo T, Benedetti JW, Brodersen CR, Castro M, Castro S, Gilbride AB, Jensen B, Jiang G-F *et al.* 2020. The scaling of genome size and cell size limits maximum rates of photosynthesis with implications for ecological strategies. *International Journal of Plant Sciences* **181**: 75–87.

Royer DL. 2001. Stomatal density and stomatal index as indicators of paleoatmospheric CO_2 concentration. *Review of Palaeobotany and Palynology* **114**: 1–28.

Sack L, Buckley TN. 2016. The developmental basis of stomatal density and flux. *Plant Physiology* **171**: 2358–2363.

Sack L, Cowan PD, Jaikumar N, Holbrook NM. 2003. The 'hydrology' of leaves: co-ordination of structure and function in temperate woody species. *Plant, Cell & Environment* **26**: 1343–1356.

Salisbury EJ. 1928. On the causes and ecological significance of stomatal frequency, with special reference to the woodland flora. *Philosophical Transactions of the Royal Society of London, Series B* **216**: 1–65.

Šímová I, Herben T. 2012. Geometrical constraints in the scaling relationships between genome size, cell size and cell cycle length in herbaceous plants. *Proceedings of the Royal Society B: Biological Sciences* **279**: 867–875.

Tsuboi M, Sztepanacz J, De Lisle S, Voje KL, Grabowski M, Hopkins MJ, Porto A, Balk M, Pontarp M, Rossoni D *et al.* 2024. The paradox of predictability provides a bridge between micro- and macroevolution. *Journal of Evolutionary Biology* **37**: 1413–1432.

Uyeda JC, Harmon LJ. 2014. A novel Bayesian method for inferring and interpreting the dynamics of adaptive landscapes from phylogenetic comparative data. *Systematic Biology* **63**: 902–918.

Vatén A, Bergmann DC. 2012. Mechanisms of stomatal development: an evolutionary view. *EvoDevo* **3**: 11.

Walsh B, Lynch M. 2018. *Evolution and selection of quantitative traits*. Oxford, UK: Oxford University Press.

Weiss AG. 1865. *Untersuchungen über die Zahlen-und Grössenverhältnisse der Spaltöffnungen*: Jahrbücher für Wissenschaftliche Botanik.

Wilson D. 1972. Effect of selection for stomatal length and frequency on theoretical stomatal resistance to diffusion in *Lolium perenne L. New Phytologist* **71**: 811–817.

Wilson D. 1975. Leaf growth, stomatal diffusion resistances and photosynthesis during droughting of *Lolium perenne* populations selected for contrasting stomatal length and frequency. *Annals of Applied Biology* **79**: 67–82.

Xie J, Fernandes SB, Mayfield-Jones D, Erice G, Choi M, Lipka E, Leakey ADB. 2021. Optical topometry and machine learning to rapidly phenotype stomatal patterning traits for maize QTL mapping. *Plant Physiology* **187**: 1462–1480.

Yoshiyama Y, Wakabayashi Y, Mercer KL, Kawabata S, Kobayashi T, Tabuchi T, Yamori W. 2024. Natural genetic variation in dynamic photosynthesis is correlated with stomatal anatomical traits in diverse tomato species across geographical habitats. *Journal of Experimental Botany* **75**: 6762–6777.

Yuan ZY, Chen HYH. 2009. Global-scale patterns of nutrient resorption associated with latitude, temperature and precipitation. *Global Ecology and Biogeography* **18**: 11–18.

Supporting Information

Additional Supporting Information may be found online in the Supporting Information section at the end of the article.

Fig. S1 The fraction of epidermal area allocated to stomata (f_S) is strongly positively correlated with the maximum stomatal conductance ($g_{s,max}$) across species of Angiosperms, Gymnosperms, and Pteridophytes.

Fig. S2 The effect of mutational variance and strength of selection on $g_{s,max}$ on the additive genetic variance within species under H_2: stomatal-area minimization hypothesis.

Fig. S3 The effect of mutational variance and strength of selection on $g_{s,max}$ on the additive genetic variance within species under H_3: stomatal adaptation + bounded size hypothesis.

Fig. S4 The effects of selection on minimizing f_S and mutational variance in stomatal size on the additive genetic variance under H_2: stomatal-area minimization hypothesis.

Fig. S5 The effects of selection on and mutational variance in stomatal size on the additive genetic variance under H_3: stomatal adaptation + bounded size hypothesis.

Fig. S6 The effect of mutational correlation between stomatal density and size on the additive genetic correlation under H_2: stomatal-area minimization hypothesis.

Fig. S7 The effect of mutational correlation between stomatal density and size on the additive genetic correlation under H_3: stomatal adaptation + bounded size hypothesis.

Fig. S8 The predicted response to selection on greater $g_{s,max}$ under three hypotheses with different mutational correlations between size and density.

Fig. S9 The predicted response to selection on greater $g_{s,max}$ under three hypotheses with different mutational variances in size and density.

Fig. S10 The predicted response to selection on greater $g_{s,max}$ under three hypotheses with different strengths of selection to minimize f_S.

Fig. S11 Among-species trait (co)variances are not sensitive to mutational ratio at stationarity.

Fig. S12 Among-species trait (co)variances are not sensitive to mutational correlation at stationarity.

Fig. S13 Among-species trait (co)variances are not sensitive to the strength of stabilizing selection on $g_{s,max}$ at stationarity.

Fig. S14 Among-species trait (co)variances are not sensitive to the strength of selection to minimize f_S at stationarity.

Fig. S15 Among-species trait (co)variances are not sensitive to the strength of stabilizing selection on stomatal size at stationarity.

Notes S1 Mathematical derivation of covariance between f_S and $g_{s,max}$.

Notes S2 Background on evolutionary quantitative genetics and estimating trait relationships.

Notes S3 Theoretical assumptions and analysis of evolutionary quantitative genetic model.

Notes S4 Evolutionary quantitative genetic simulations.

Table S1 Glossary of mathematical symbols.

Table S2 Range of parameter values for numerically solving within species genetic covariance under H_2.

Table S3 Range of parameter values for numerically solving within species genetic covariance under H_3.

Please note: Wiley is not responsible for the content or functionality of any Supporting Information supplied by the authors. Any queries (other than missing material) should be directed to the *New Phytologist* Central Office.